Ryszard STRZELECKI[1,3], Wojciech MATELSKI[2], Valentin TOMASOV[3]

Gdańsk University of Technology (1), Electrotechnical Institute, Warsaw (2),
ITMO University, Sankt Petersburg (3) Russian Federation

doi:10.15199/48.2018.06.23

Hybrid stepless distribution transformer with four-quadrant AC/DC/AC converter at low voltage side - simulation tests

***Abstract**. The article presents the work of the stepless hybrid distribution transformer (HT), as an alternative to the so far applied Automatic Voltage Regulator (AVR) solutions, used to control the voltage in the power system in terms of the fundamental harmonic. The HT is a combination of a conventional distribution transformer and an AC/DC/AC converter connected in series with the transformers secondary winding. In the work the basic control algorithm of the AC/DC/AC converter operated as a series connected additive voltage source in the HT system, has been described. The article contains the preliminary results of computer simulation studies of the model elaborated in PSIM.*

***Streszczenie.** W artykule opisano działanie bezstopniowego hybrydowego transformatora dystrybucyjnego (HT), jako alternatywę dla dotychczas stosowanych rozwiązań AVR (Automatic Voltage Regulator), służących do kontroli poziomu napięcia w systemie elektroenergetycznym w zakresie podstawowej harmonicznej. Układ HT to połączenie konwencjonalnego transformatora dystrybucyjnego oraz przekształtnika AC/DC/AC włączonego w szereg z uzwojeniem wtórnym transformatora. W pracy przedstawiono podstawowy algorytm sterowania przekształtnikiem AC/DC/AC jako szeregowe źródło napięcia dodawczego w układzie badanego HT. Artykuł zawiera wstępne wyniki badań symulacyjnych modelu opracowanego w programie PSIM. (**Hybrydowy bezstopniowy transformator dystrybucyjny z czterokwadrantowym przekształtnikiem AC/DC/AC po stronie niskiego napięcia – badania symulacyjne**).*

Keywords: hybrid distribution transformer, automatic voltage regulator, power distribution, power transformers.
Słowa kluczowe: hybrydowy transformator dystrybucyjny, automatyczny regulator napięcia, dystrybucja mocy, transformatory mocy.

Introduction

The present energy distribution grid is in operation for decades and works with the same principles since its establishment [1]. This grid was designed to supply linear loads, i.e. light bulbs or heaters. For such devices the power drawn from the grid decreases together with the voltage, mitigating the negative effects of lowering the voltage.

In recent years the operating conditions of the distribution grid have changed. Most of modern loads work with constant power demand. In such cases the decrease of the voltage causes an increase of the current drawn, which intensifies the problems occurring in the distribution systems. The change of grid operation conditions is also the effect of the work of distributed generation systems, with a large contribution of renewable energy sources (RES). The increasing number of dynamic loads, i.e. fast charging stations for electric vehicles (EV) are also a reason of this issue. As a result, increasing voltage fluctuations in the grid become more severe.

In order to control the voltage level, conventional distribution transformers (DT) are complemented by various Automatic Voltage Regulator (AVR) devices, starting from electromechanical servomechanisms, through transformer tap changers (TC), to Solid State Transformers (SST) [1-4]. Currently, despite such disadvantages like arcing, high operation costs or poor dynamics, mechanical tap changers are the most common solution. However this AVR technology does not keep up with the present grid voltage regulation requirements, especially in terms of dynamics and accuracy, anymore. This is the fundamental reason behind the growth in the application of power electronic based AVR devices.

Thyristor tap changers (DT+TC) [4-6], although operating on a similar principle as their mechanical versions, they eliminate arc problems and guarantee higher dynamics of regulation. These switches, however, still operate in a step manner, and the indicated decrease in step value is associated with a significant increase of the costs (Fig.1). With a high number of taps the validity of such a solution is questionable. The broadest regulatory and functional capabilities of the AVRs provide SST based solutions [4, 7, 8]. Nevertheless, costs and losses in this case are approximately 4 times and 3 times higher, than for the standard DT transformer (Fig.1). Therefore, the use of SST systems in the AC grid has not been yet sufficiently justified.

A competitive alternative to the presented above AVR solutions, are hybrid transformers (HT) [9], combining the features of a conventional transformer and the regulatory capabilities of modern power converters. In this case, the converter, enabling smooth and instantaneous voltage adjustment, is designed to convert only a fraction of the transferred power. What is more, in the event of converter failure, the energy can still be transferred to the load, so that reliability of the power supply is ensured. The use of HT systems, combining high efficiency and low cost of DT, with high functionality of power converters (Fig.1), fully meets the requirements of modern AVR, such as:

- fast voltage correction (within 20 ms),
- precise output voltage regulation as a percentage of the rated supply voltage,
- high: efficiency, reliability and safety during faults,
- low impedance in order to mitigate the effect of load changes,
- continuous power supply during switch operations.

The main purpose of this article is to present the basic control algorithm and the simulation study results of the HT with stepless voltage regulation in the ±10% range. The system is made up of a standard distribution transformer with an additional, tertiary winding and a voltage control AC/DC/AC converter. The studies, illustrating and enabling the evaluation of the properties of the selected HT configuration, are the preliminary part of a project, carried out by the Electrotechnical Institute in a consortium with the industry. The secondary objective is to evaluate the selected solution against alternative HT configurations with continuous voltage regulation.

Power electronics systems similar to hybrid transformers were investigated since the 70s of the 20th century. As fully controllable high-power switches, forced-commutated thyristors were used. In this area, in Poland, pioneering works were those conducted by prof. Antoni Dmowski [6] and his team, including prof. Jan Mućko, his doctoral student. Thyristor technology has, however, significantly hindered the construction, and thus limited the use, of

switch mode AC regulators. The trigger for the further development of such devices was the widespread application of power transistors. New concepts of systems and control algorithms [10, 11] have been introduced, utilizing mainly the basic topologies of AC choppers. Later, other AC/AC chopper topologies [12-14], and even matrix converters [15], were proposed. These solutions, so far, have not found industrial approval. One of the reasons is the need for AC switches, which create EMC problems, commutation stress and increased switching losses. What is more, in direct AC/AC converters, the instantaneous active power values at the input and output are equal, which limits the functionality of these converters (the impact on network voltage parameters).

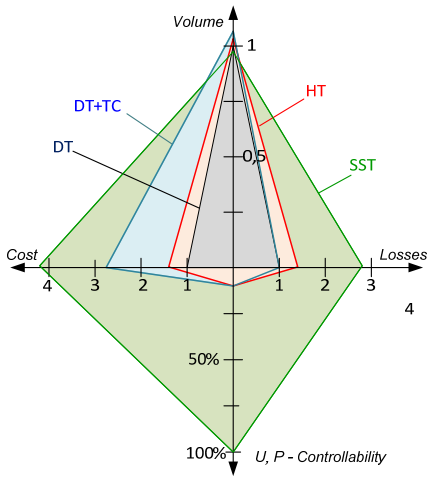

Fig.1. Comparison of volume, losses, cost and controllability for power electronic arrangements of AVR technology referenced to standard distribution transformer [9]

HT systems are devoid of the above mentioned disadvantages. The regulator function is satisfied by the back-to-back voltage converter [9, 16]. This feature makes it possible to separate a DC circuit, which can be the connection point for energy storage or DC sources, e.g. PV panels. The HT system also allows for double, series and parallel compensation, which gives similar properties as the Universal Power Quality Controller (UPQC) [17]. The difference mainly concerns the range of network voltage regulation and current compensation, that determine the power of the inverter. In the case of the distribution HT the range is 10% of the nominal voltage rating. Hence, one of the most important problems, although not covered by this article, is the proper protection of HT [18].

Hybrid transformer realization

In principle, two basic concepts of the construction of hybrid transformer systems, can be distinguished (Fig.2). The advantage of the first concept (Fig.2a) are the low currents and no converter neutral wire. On the other hand, in the case of U_{MV} = 15kV (Fig.2b), the voltage of the inverters DC circuit requires a voltage level of about 2,3-2,4 kV, which necessitates the use of high-voltage transistors. Therefore, the PWM carrier frequency will be less than in the second concept (Fig. 1b). From this reason, and because it is more difficult for the system presented in figure 2a to implement the protection infrastructure, the HT structure with the converter on the transformer primary side is not the subject of the presented study.

The functionality of the stepless hybrid transformer has been presented and investigated on an exemplary structure depicted in figure 2b. In PSIM v10 simulation software the HT model has been elaborated. A relatively simple control system, suited for balanced loads, has been implemented, providing regulation and stabilization of the load voltage fundamental harmonic. The presented research is the first step in the optimization process of the HT parameters and in the selection and development of the optimal control algorithm.

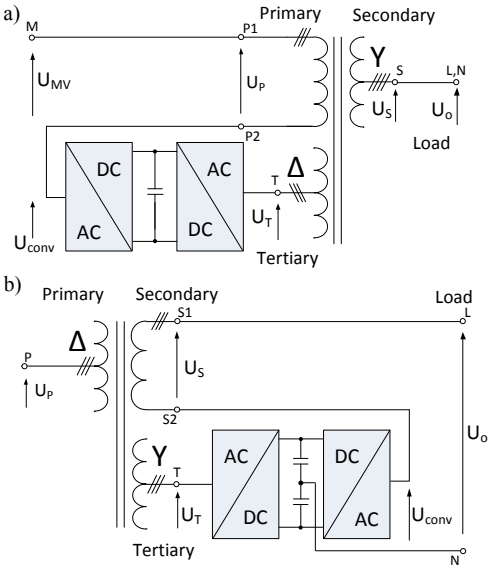

Fig.2. Hybrid transformer concepts: a) converter placed on DT medium voltage side; b) converter placed on DT low voltage side

In the chosen HT structure the power electronic converter is situated on the low voltage side of the distribution transformer DT. Thus, for the realization of the AC/DC and DC/AC parts of the converter, enabling the stepless load voltage U_o regulation, the 2-level three phase voltage source inverter structures in back-to-back configuration were selected.

The AC/DC part (Fig.2b), working in rectifier mode (conventionally – both parts enable bidirectional power flow) is connected to the beginnings of the dedicated tertiary winding (T) of the DT and will be referred to as Tertiary Side Converter (TSC). The endings of the T winding are short-circuited and form the star-point of the tertiary winding. The inverter DC/AC part is series connected, to the S2 terminals, with the secondary winding (S), and will be referred to as Secondary Side Converter (SSC). The middle point of the DC voltage circuit is the star-point of the DT secondary winding. This potential has to be led out to the load, in form of a neutral wire N, in order to power single phase, 230 V RMS devices. Due to the DT's winding configuration (D/Y) the zero voltage component is not transferred from the P to the S winding. Therefore in the preliminary simulated cases the zero voltage component control loop was not included in the HT control system.

The SSC and TSC parts are controlled separately, wherein the TSC converter is responsible for the regulation of the U_{dc} voltage of the DC circuit, whereas the SSC part generates the voltage U_{conv} added (geometrically) to the main secondary winding S voltage U_S, to regulate and stabilize the load voltage U_o of the HT. Therefore, the output HT voltage equals:

$$\underline{U_o} = \underline{U_S} + \underline{U_{conv}} \tag{1}$$

where: the underlined voltages are complex values.

The control system, in form of a block diagram, is depicted in figure 3. The blocks LPF1 and LPF2 stand for low-pass filters, which are an integral part of the HT. In the simulated circuit lossless models of semiconductor devices were used.

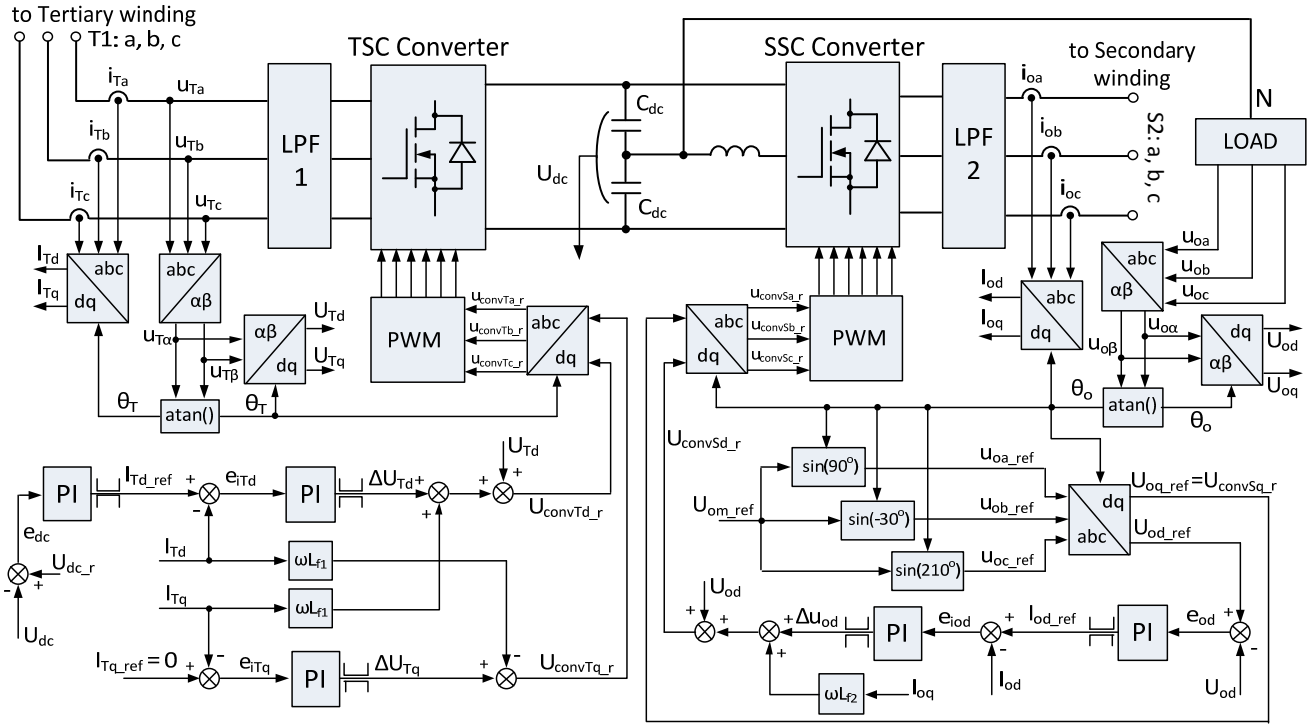

Fig.3. Hybrid transformer simplified converter control system block diagram

An indispensable element of the HT is a specialized switch, which enables bypassing of the SSC converter, so that the HT can work as a conventional distribution transformer, and the load is powered solely from the secondary winding. The bypass switch is the main protection device in situations of faults, such as overvoltages or short circuits, and it is not the subject of this article.

Distribution transformer model

In the simulated HT circuit the three-phase three winding 600 kVA 15/0,4 kV distribution transformer is represented by the dedicated *3-ph 3-w Transformer* block available from the PSIM software library [19]. The additional winding T, rated for only a fraction of the DT primary winding power, is dedicated for the TSC converter. The rated values, the model should resemble, and winding configurations, are listed in table 1.

The calculated DT equivalent circuit parameters, entered into the simulation block, are referred to its primary side and are listed in table 2. The short circuit parameters and magnetizing current are presented in table 3.

HT control strategy

TSC control scheme

The TSC part of the converter works as a PWM rectifier, controlled with the principles of the well-known Voltage Oriented Control – VOC scheme [20]. The control system was implemented in the orthogonal d-q coordinate frame, synchronously rotating with the T winding voltage space vector. The angle of this vector, denoted as Θ_T, is calculated on the basis of the measurements of the phase voltages: u_{Ta}, u_{Tb}, u_{Tc}. The given three phase voltage system is transformed to the stationary, two-phase coordinate system, using the Clarke transformation, so that the $u_{T\alpha}$ and $u_{T\beta}$ components are calculated. The position of the tertiary winding voltage vector, with respect to the α-axis - Θ_T, is calculated from:

$$\Theta_T = arctg\left(\frac{u_{T\beta}}{u_{T\alpha}}\right) \tag{2}$$

With the knowledge of Θ_T the Park transformation is possible, and the rotating d-q frame components u_{Td} and u_{Tq} are calculated. The d-axis is aligned with the T winding voltage vector, thus u_{Tq} equals 0.

Table 1. Three phase, three winding transformer rated values

Parameter	Winding		
	Primary: P	Secondary: S	Tertiary: T
U_{xn}	15 kV	400 V	40 V
U_{xfn}	15 kV	230 V	23 V
f_n	50 Hz		
Winding config.	D	y*	y
S_{xn}	600 kVA	600 kVA	60 kVA
I_{xfn}	23,04 A	866,03 A	866,03 A
N_x	650	10	1

$x \in$ {P, S, T}; U_{xn} – phase to phase voltage; U_{xfn} – phase voltage; f_n – frequency of U_{xn}; S_{xn} – apparent power; I_{xfn} – phase current; N_x – number of turns; * - winding star point is formed by the converter DC neutral point.

Table 2. Three phase, three winding transformer equivalent circuit parameters referred to primary side

Parameter	Winding		
	P	S	T
R_x [Ω]	3	10	29
L_{lx} [H]	0,085	0,113	0,17
L_m [H]	17		

R_x – winding resistance; L_{lx} – leakage inductance; L_m – magnetizing inductance.

Table 3. Three phase, three winding transformer short-circuit parameters and magnetizing current

x-y	$U_{scx\text{-}y}$ [V]	$U_{scx\text{-}y}$ [%]	$R_{scx\text{-}y}$ [Ω]	$X_{scx\text{-}y}$ [Ω]	I_{oP} [A]	$I_{oP\%}$ [%]
P-S	1468	9,79	13	62,204	1,87	8,116
P-T	1990	13,27	32	80,111		
S-T	38,4	9,60	0,0092	0,021		

U_{sc} – short-circuit voltage; R_{sc} – short circuit resistance; X_{sc} – short circuit reactance; I_o – magnetizing current.

In the T winding three currents are measured: i_{Ta}, i_{Tb}, i_{Tc}, which after filtering the high frequency components, are transformed directly to the rotating d-q frame system (also synchronously rotating with the T winding voltage space vector), by the use of the Clarke-Park transformation. The value of the angle Θ_T is used and as a result, the components I_{Td}, I_{Tq} are obtained.

In the outer TSC control loop the DC link voltage U_{dc} of the converters is regulated. The output signal of the PI controller is the d-axis reference current I_{Td_ref}. The active power of the TSC converter is proportional to the value of I_{Td}. Through setting the reference current value in the q-axis on 0, the current of the T winding is in phase with the voltage (or counter phase, when I_{Td} < 0), thus unity power factor operation is achieved. The TSC converter exchanges with the grid active power only.

In order to ensure high dynamic operation, decoupled PI current controllers have been applied. The control loops output signals $U_{convT\_d\_r}$ and $U_{convT\_q\_r}$, used in the later PWM signal generation, are described by the equations:

(3) $$U_{convTd\_r} = \omega_T L_{f1} I_{Tq} + U_{Td} + \Delta U_{Td}$$

(4) $$U_{convTq\_r} = -\omega_T L_{f1} I_{Tq} + \Delta U_{Tq}$$

where: ΔU_{Td}, ΔU_{Tq} - output signals of the current controllers, L_{f1} – inductance of the low-pass filter LPF1 [H].

The result command values are directly transformed to the natural a-b-c system with the inverse Clarke-Park transform. The calculated u_{convTa_r}, u_{convTb_r}, u_{convTc_r} signals are sent to the PWM modulator (sinusoidal modulation with triangle 20 kHz carrier frequency signal).

SSC control scheme

The SSC part of the system, series connected with the secondary S winding, is used to regulate the load voltage within the +/-10% limits of the nominal 400 V phase-to-phase voltage. The load phase voltages u_{oa}, u_{ob}, u_{oc} are measured: and transformed to the α-β coordinate system (Clarke transformation), so that the $u_{o\alpha}$ i $u_{o\beta}$ components are calculated. Thus, the angle Θ_o of the load voltage space vector is obtained:

(5) $$\Theta_o = arctg\left(\frac{u_{o\beta}}{u_{o\alpha}}\right)$$

With the knowledge of this angle, the α-β voltage components are transformed, according to the Park transformation, to the rotating reference frame, and the U_{od} and U_{oq} values are calculated.

In the system three load currents (i_{oa}, i_{ob}, i_{oc}) are measured and transformed directly to the rotating d-q reference frame, using the Clarke-Park transformation. In this way, the I_{od} and I_{oq} components are obtained.

The reference load phase voltage values are calculated according to equations:

(6) $$u_{oa\_ref} = U_{om\_ref} \sin(\Theta_o + \frac{\pi}{2})$$

(7) $$u_{ob\_ref} = U_{om\_ref} \sin(\Theta_o + \frac{\pi}{2} - \frac{2\pi}{3})$$

(8) $$u_{oc\_ref} = U_{om\_ref} \sin(\Theta_o + \frac{\pi}{2} + \frac{2\pi}{3})$$

where: U_{om_ref} – load phase voltage reference amplitude [V].

The reference values are directly transformed to the d-q frame, rotating synchronously with the load voltage space vector, thus U_{od_ref} and U_{oq_ref} are calculated. The d-axis is aligned with the load voltage space vector, hence the command voltage q-axis value of the SSC converter U_{oq_ref} is 0. The additive voltage generated by the SSC converter is in phase with the load voltage, and its regulation is performed only in the d-axis control loop. The outer U_{od} voltage PI regulator generates the reference I_{od_ref} current value. The converter command values are calculated according to equations:

(9) $$U_{convSd\_r} = \omega_o L_{f2} I_{oq} + U_{od} + \Delta U_{od}$$

(10) $$U_{convSq\_r} = 0$$

where: ΔU_{od} – d-axis current controller output value; L_{f2} – inductance of the low-pass filter LPF2 [H].

The result command values are directly transformed to the natural a-b-c system with the inverse Clarke-Park transform. The calculated u_{convSa_r}, u_{convSb_r}, u_{convSc_r} signals are sent to the PWM modulator (sinusoidal modulation with triangle 20 kHz carrier frequency signal).

Simulation results

The performance of the system was tested for four characteristic events, occurring in the grid.

At first, the response of the HT to step changes of the voltage at the primary side of the distribution transformer was tested. This was achieved through the use of controlled voltage sources, generating 50 Hz symmetric three-phase sinusoidal voltages: U_{PA}, U_{PB}, U_{PC}, connected to the transformer P windings. During the simulation there was a step change of the RMS value U_P of these voltages:

- for ($t \le 0{,}1$ s) $U_P = U_{Pn}$ = 15000 V;
- for (0,1 s < $t \le 0{,}2$ s) $U_P = 0{,}9U_{Pn}$ = 13500 V;
- for (t > 0,2 s) $U_P = 1{,}1U_{Pn}$ = 16500 V;

The system was supposed to maintain the load voltage on its nominal level, equal 230 V RMS, hence the reference amplitude was set at: U_{om_ref} = 325 V (conf. eq. 6, 7, 8). At the beginning of the simulation, the current in the S winding did not flow. After 0,05 s the load switch was closed. After this event, between the terminals L of the S winding and the neutral wire N, the symmetric three-phase load was turned on (series per-phase R_o-L_o connection), which equaled: R_o = 0,5 Ω; L_o = 0,35 mH; cosϕ_o = 0,98. The results of the simulation, in the form of selected waveforms, are presented in figures 4 – 10.

In the second case, the response of the HT to abrupt changes of the load impedance, in conditions of constant primary side supply voltage U_P, was tested. During the simulation the load was changed as follows (per-phase values, connected between the L-N terminals):

- for ($t \le 0{,}1$ s): R_o = 0,64 Ω; L_o = 1 mH; cosϕ_o = 0,9
- for (0,1 s < $t \le 0{,}2$ s): R_o = 0,32 Ω; L_o = 1 mH; cosϕ_o = 0,71
- for (t > 0,2 s): R_o = 0,64 Ω; L_o = 1 mH; cosϕ_o = 0,9

The results are presented in figures 11 – 17.

In the third simulation the event of unbalanced voltages of the grid has been presented. A 10% voltage dip in phase A of the supply phase voltage U_A (three phase voltage sources U_A, U_B, U_C: Y-connected) was prepared, so the phase voltages (RMS) were: U_A = 7794 V; U_B = 8660 V; U_C = 8660 V. During the test the load impedance was constant and equaled (per phase): R_o = 0,55 Ω; L_o = 0,35 mH; cosϕ_o = 0,981. The results presenting the response of the system in steady state conditions are depicted in figures 18 – 25.

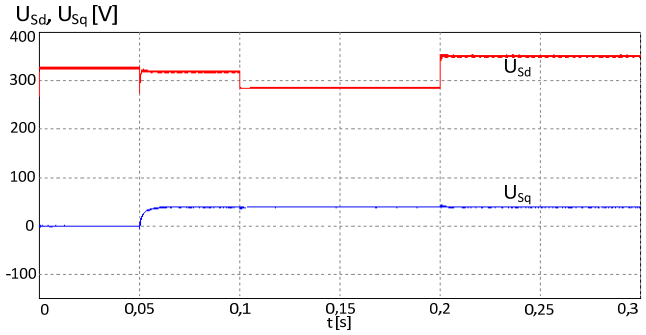

Fig.4. Transformer secondary side voltages in d-q frame U_{Sd}, U_{Sq}

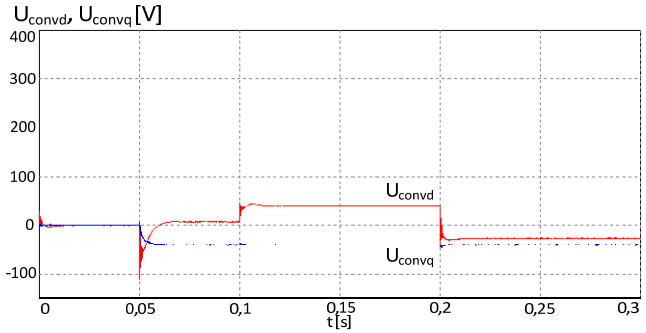

Fig.5. SSC converter voltages in d-q frame voltage U_{convd}, U_{convq}

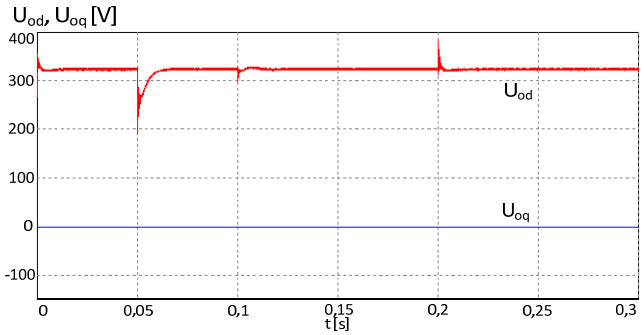

Fig.6. Load voltages in d-q frame U_{od}, U_{oq}

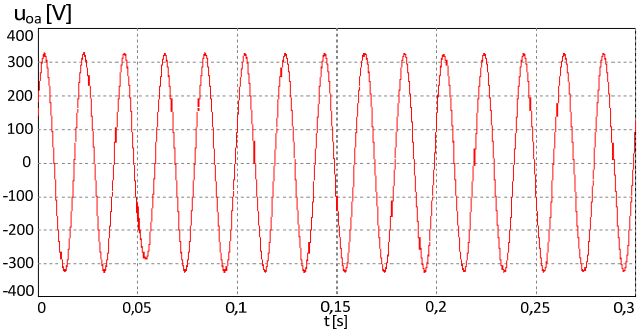

Fig.7. Load phase a voltage u_{oa}

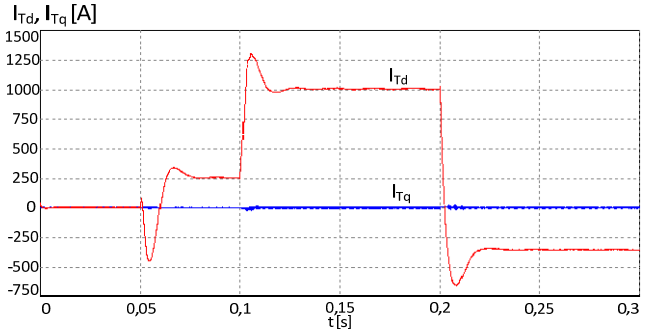

Fig.8. Tertiary winding d-q frame currents: I_{Td}, I_{Tq}

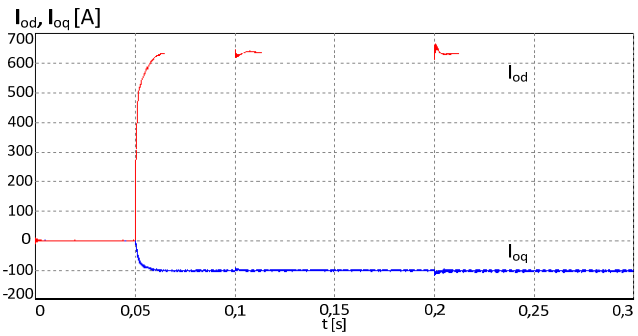

Fig.9. Load current d-q frame components: I_{od}, I_{oq}

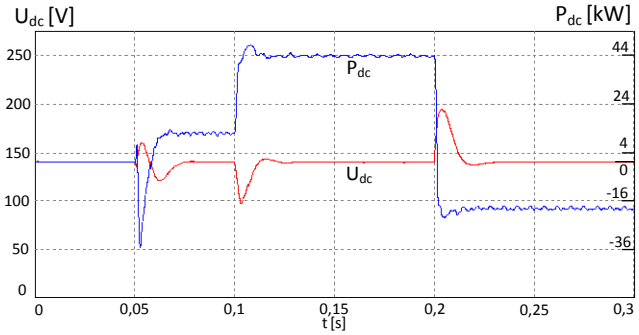

Fig.10. Converter SSC DC link voltage U_{dc} and active power P_{dc}

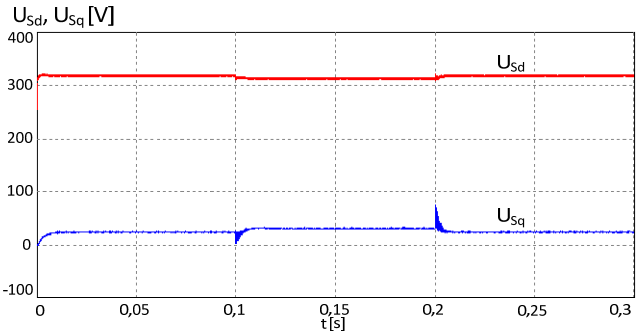

Fig.11. Transformer secondary side voltages in d-q frame U_{Sd}, U_{sq}

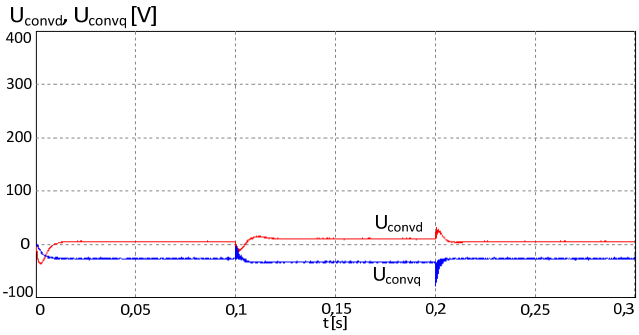

Fig.12. SSC converter voltages in d-q frame voltage U_{convd}, U_{convq}

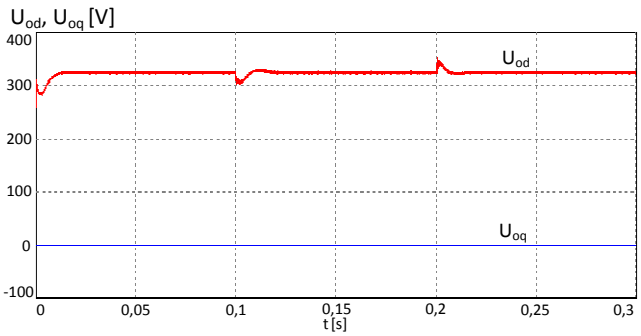

Fig.13. Load voltages in d-q frame U_{od}, U_{oq}

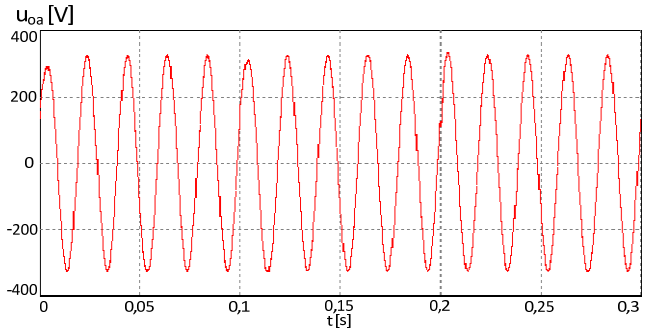

Fig.14. Load phase a voltage u_{oa}

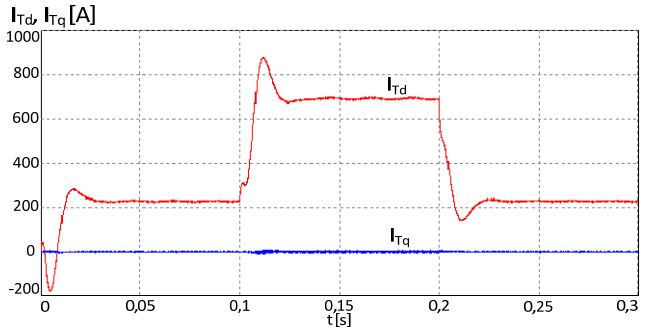

Fig.15. Tertiary winding d-q frame currents: I_{Td}, I_{Tq}

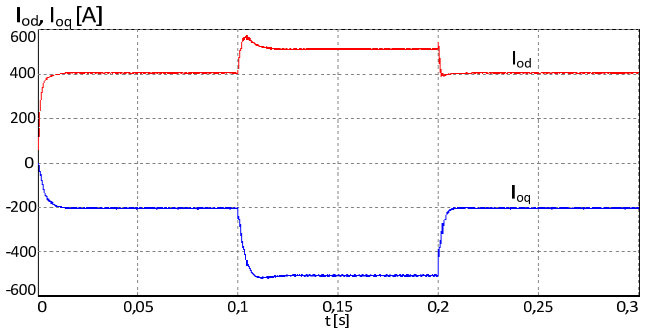

Fig.16. Load current d-q frame components: I_{od}, I_{oq}

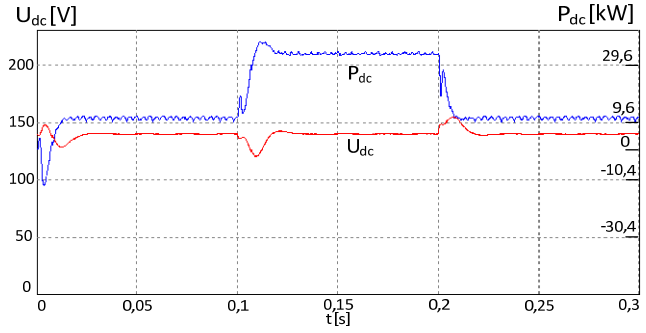

Fig.17. Converter SSC DC link voltage U_{dc} and active power P_{dc}

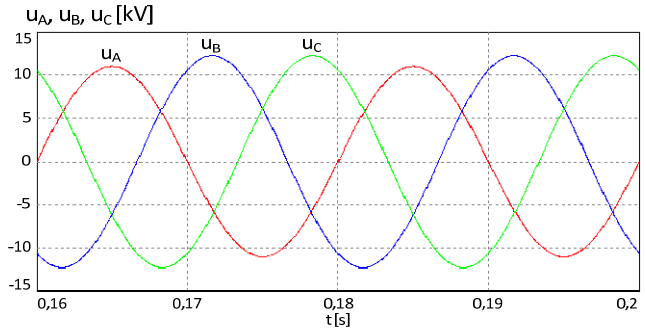

Fig.18. Grid (MV) phase voltages: U_A, U_B, U_C

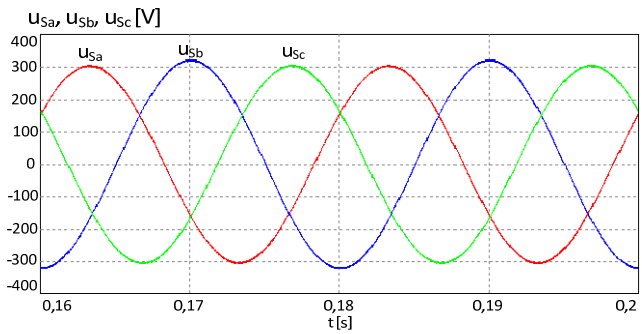

Fig.19. DT S-winding phase voltages: u_{Sa}, u_{Sb}, u_{Sc}

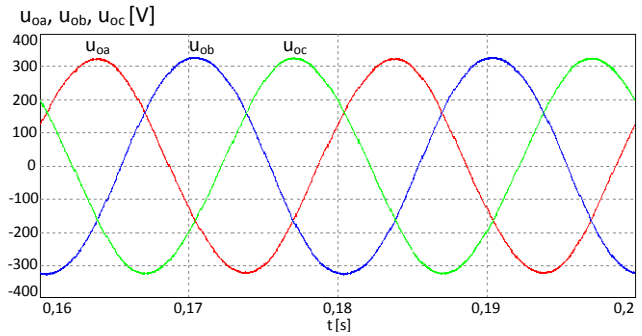

Fig.20. Load phase voltages: u_{oa}, u_{ob}, u_{oc}

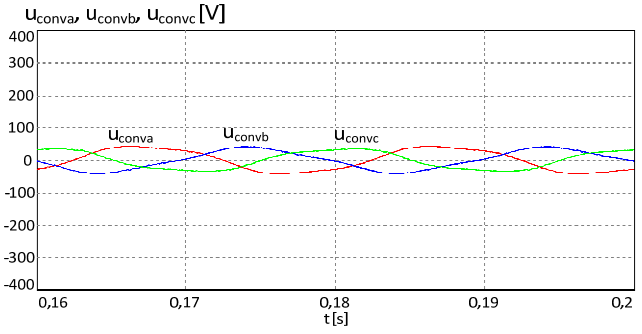

Fig.21. SSC Converter output voltages: u_{conva}, u_{convb}, u_{convc}

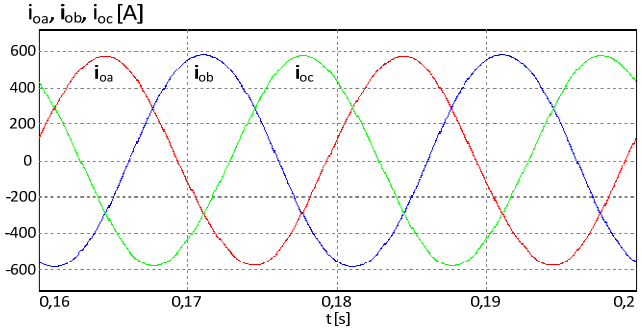

Fig.22. Load phase currents: i_{oa}, i_{ob}, i_{oc}

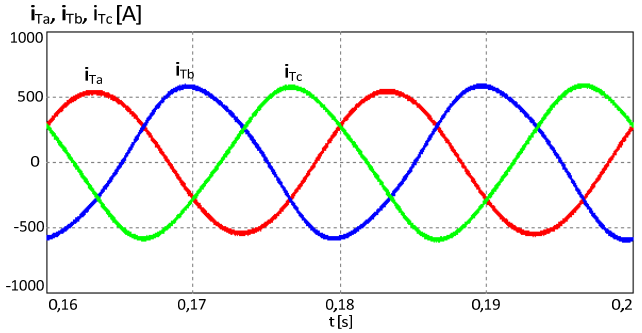

Fig.23. Tertiary winding phase currents: i_{Ta}, i_{Tb}, i_{Tc}

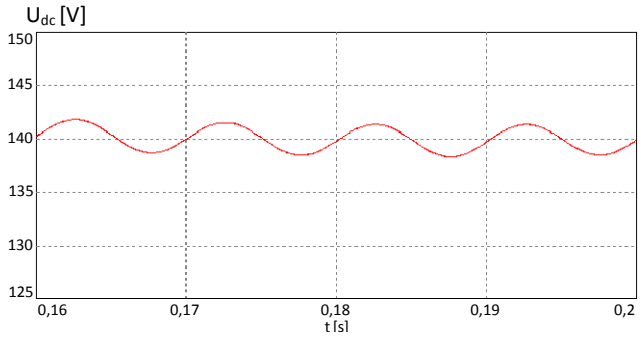

Fig.24. Converter SSC DC link voltage U_{dc}

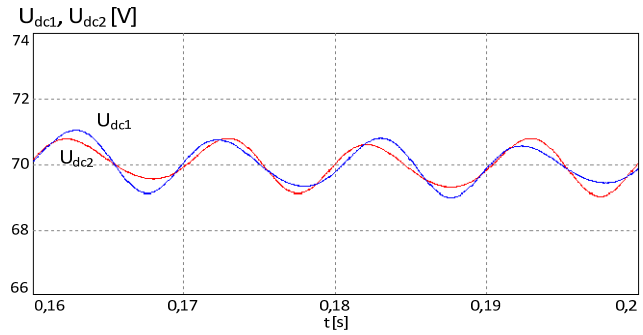

Fig.25. Converter DC link voltage components U_{dc1}, U_{dc2}

Conclusion

The operating conditions of the power system change rapidly. As a result voltage fluctuations in the grid become severe. In the future this problem is expected to grow, and the current AVR solutions may not be sufficient.

In the article the work of the stepless hybrid distribution transformer, combining the features of a conventional low frequency transformer with the regulatory capabilities of modern power converters, was described. This idea meets the requirements of modern AVR devices and is an attractive and competitive alternative in terms of price and reliability, to the currently intensively studied SST solutions.

The presented HT basic control algorithm and elaborated model were tested in form of simulation studies. The preliminary results show proper operation in situations of variation of the supply voltage, load impedance, and load switch operations. The system was able to restore the load voltage to the command nominal value in times below 20 ms and maintain it on the desired level. The presented structure was also tested in terms of Primary side supply voltage unbalance. During steady state operation the HT ensures the balance between the load phase voltages.

Due to the high DT short-circuit power (with respect to its nominal power, conf. Tab.1 and Tab.3) no significant impact of unsymmetrical loads on the DT S-side voltages was found. Currently research related to DTs with lower short-circuit power (max. 4 to 5 times greater than the DT's nominal power) is being conducted. The results will be published in subsequent articles.

The presented research is the preliminary part of a project, carried out by the scientific-researches consortium in cooperation with the industry, aimed at the development of the optimal HT structure and control algorithm. The research is still underway.

***Authors**: prof. Ryszard Strzelecki, E-mail: profesor1958@gmail.Com, Gdańsk University of Technology, Narutowicza 11/12, 80-233 Gdańsk, mgr inż. Wojciech Matelski, E-mail: wojciech.matelski@iel.pl; Instytut Elektrotechniki, Bałtycka Pracownia Technologii Energoelektronicznych ul. Czechosłowacka 3, 81-336 Gdynia; prof. Valentin Tomasov, E-mail: tomasov@ets.ifmo.ru; ITMO University, 197101, Sankt Petersburg, Kroneverkskiy pr.49.*

REFERENCES

[1] Strzelecki R., Benysek G., Power Electronics in Smart Electrical Energy Networks, *London: Springer,* (2008), 414

[2] Matsuda K., Horikoshi K., Seto T., Iyama O., Kobayashi H., Development of Automatic Voltage Regulator for Low-Voltage Distribution Systems. Electrical Engineering in Japan, 188 (2014), No.4, 9-19

[3] Lopez J.V, Garcia S.M, Rodriguez J.C., Garcia R.V., Fernandez S.M., Olay C.C., Electronic Tap-Changing Stabilizers for Medium-Voltage Lines Optimum Balanced Circuit, *IEEE Trans. on Power Delivery*, 27 (2012), No. 4, 1909-1918

[4] She X., Huang A.Q., Burgos R., Review of Solid-State Transformer Technologies and Their Application in Power Distribution Systems, *IEEE Journal of Emerging and Selected Topics in Power Electronics*, 1 (2013), No.3, 186-198

[5] Липковский К.А., Трансформаторно-ключевые исполнительные структуры преобразователей переменного напряжения. *Изд. Наук. думка, Киев*, (1983), 214

[6] Dmowski A., Tyrystorowe regulator napięć przemiennych, *Wydawnictwa Politechniki Warszawskiej* (1979), 113

[7] Roasto I., Strzelecki R., "A simple modular active power electronic transformer," *IEEE 23rd International Symposium on Industrial Electronics –(ISIE'14)*, Istanbul (2014), 1976-1980

[8] Huang A.Q., Medium-Voltage Solid-State Transformer: Technology for a Smarter and Resilient Grid, *IEEE Industrial Electronics Magazine*, 10 (2016), No. 3, 29-42.

[9] Burkard J., Biela J., Evaluation of topologies and optimal design of a hybrid distribution transformer, Proc of the *17th European Conference on Power Electronics and Applications (EPE'15 ECCE-Europe),* Geneva (2015), 1-10.

[10] Gołubiew V., Lipkowskij K., Mućko J., Strzelecki R., Środki zwiększenia efektywności regulatorów impulsowych napięcia przemiennego. *Zeszyty Nauk. ATR Bydgoszcz – Elektrotechnika,* 11 (1995), nr 191, 41-48

[11] Do-Hyun Jang, Gyu-Ha Choe, Step-Up/Down AC Voltage Regulator using Transformer with Tap Changer and PWM AC Chopper. *IEEE Transactions on Industrial Electronics*, 45 (1998), No. 6, 905-911

[12] Z. Fedyczak, R. Strzelecki, K Sozański, Review of three-phase PWM AC/AC semiconductor transformer topologies and applications. *Symposium "SPEEDAM"*, Ravello-Naples, (2002), B5.19—24

[13] Z. Fedyczak, R. Strzelecki, Single-phase PWM AC/AC semiconductor transformer topologies and applications. *IEEE 33rd Annual IEEE Power Electronics Specialists Conference (PESC'02)*, Cairns, Vol. 2, (2002), 1048-1053

[14] J. Kaniewski J., Fedyczak Z., Łukiewski M, Implementacja trójfazowego transformatora hybrydowego ze sterownikiem matrycowym. *Przegląd Elektrotechniczny*, 86 (2010), nr 2,231-236

[15] Szcześniak P., Kaniewski J., Hybrid Transformer With Matrix Converter, *IEEE Trans. on Power Delivery*, 31 (2016), No. 3, 1388-1396

[16] Mohamed Y. Haj-Maharsi M.Y., Bala S., Hybrid Distribution Transformer with an Integrated Voltage Source Converter. *Patent Application Publication*., Pub. No.: US 2010/0220499 A1 (2010), 1- 32

[17] Strzelecki R., Właściwości trójfazowego układu UPQC – modelowanie i weryfikacja eksperymentalna. *Przegląd Elektrotechniczny*, 81 (2005), nr 11, 27-18

[18] Burkard J., Biela J., Protection of hybrid transformers in the distribution grid, Proc. of the *18th European Conference on Power Electronics and Applications (EPE 16, ECCE Europe*), Karlsruhe (2016), 1-10

[19] PSIM User's Guide, Version 10.0, Release 5, Powersim Inc, January (2016)

[20] Kaźmierkowski M. P., Blaabjerg F., Malinowski M., Control in Power Electronics: Selected Problems, Academic Press, Boston (2002)